Journal of Inflammation Research

Dovepress
Taylor & Francis Group

Open Access Full Text Article

ORIGINAL RESEARCH

The Different Immune Response Between Onset and Remission of AQP4 Antibody-Positive Optic Neuritis Based on RNA Sequencing of Whole Blood

Ruohan Shi[1,*], Yidan Luo[2,3,*], Yusheng Chen[1,2,*], Xuelian Chen[4], Shiyi Li[5], Ziqing Chen[1], Ke Wang[6,7], Wenjun Zou[1,2]

[1]Department of Ophthalmology, Wuxi No.2 People's Hospital, Jiangnan University Medical Center(JUMC), Wuxi, Jiangsu, People's Republic of China; [2]Department of Ophthalmology, Affiliated Wuxi Clinical College of Nantong University, Wuxi, Jiangsu, People's Republic of China; [3]Department of Comprehensive Ophthalmology, Wuhan Bright Eye Hospital, Wuhan, Hubei, People's Republic of China; [4]Department of Ophthalmology, PuNan Branch of Ren Ji Hospital, School of Medicine, Shanghai Jiao Tong University, Shanghai, People's Republic of China; [5]Department of Ophthalmology, Jingjiang People's Hospital Affiliated to Yangzhou University, Taizhou, Jiangsu, People's Republic of China; [6]National Health Commission (NHC) Key Laboratory of Nuclear Medicine, Jiangsu Key Laboratory of Molecular Nuclear Medicine, Jiangsu Institute of Nuclear Medicine, Wuxi, Jiangsu, People's Republic of China; [7]Department of Radiopharmaceuticals, School of Pharmacy, Nanjing Medical University, Nanjing, Jiangsu, People's Republic of China

*These authors contributed equally to this work

Correspondence: Wenjun Zou, Department of Ophthalmology, Wuxi No.2 People's Hospital, Jiangnan University Medical Center (JUMC), Wuxi, Jiangsu, People's Republic of China, Tel +86-510-6856-3091, Fax +8668562052, Email wenjunzou2022@163.com

Purpose: We aimed to investigate differences in the immune response between the onset and remission phases of AQP4 antibody-positive optic neuritis (AQP4-ON).

Methods: Whole blood samples were collected from 7 healthy volunteers, 6 patients with AQP4-ON in the acute phase and 6 patients with AQP4-ON in the remission phase. Gene expression patterns and immune response pathways associated with the disease phases were identified by sequencing the RNA. CIBERSORTx was used to identify infiltrated immune cells.

Results: The enrichment analysis showed that Toll-like receptors, cytokine activity and neutrophil-mediated immune activity were significantly enriched in the acute phase, whereas cell cycle pathway was significantly enriched in the remission phase. *TSPO* and *CDK1* were the core genes in the acute and remission phases, respectively. *TSPO* expression was positively correlated with M0 macrophages and neutrophils, whereas it was significantly negatively correlated with CD8 T cells (rs=0.66, P=0.0195) and resting natural killer (NK) cells (rs=0.6662, P=0.0180). Best corrected visual acuity (BCVA; logMAR) was positively correlated with activated CD4 memory T cells and resting NK cells and negatively correlated with neutrophils in the acute phase. BCVA (LogMAR) was negatively correlated with monocytes, CD8 T cells, and M0 macrophages and positively correlated with neutrophils in the remission phase.

Conclusion: The present findings provide valuable insights into different immune responses during different phases of AQP4-ON, which is helpful for patients to develop targeted therapies and personalized treatment strategies.

Keywords: AQP4 antibody-positive optic neuritis, RNA sequencing, immune response, inflammation, gene expression

Introduction

Optic neuritis (ON), an inflammatory condition, affects the optic nerve, thereby causing blurred vision, eye pain, and potential vision loss.[1,2] AQP4 antibody seropositive ON (AQP4-ON), a relatively rare autoimmune inflammatory disorder of the optic nerve, is generally considered a subtype of neuromyelitis optica spectrum disorder (NMOSD), a condition characterized by recurrent ON and myelitis episodes.[3,4] AQP4-ON prevalence is estimated to be around 1—4 cases per 100,000 individuals,[5,6] which are more commonly found in populations of East Asian, African, and Hispanic

Received: 16 January 2025
Accepted: 23 July 2025
Published: 30 July 2025

descent.[7] AQP4-ON pathogenesis involves autoimmune reactions against AQP4 antibodies that cause demyelination, complement-mediated astrocyte lysis, and subsequent nerve signaling impairment. This inflammatory process includes multiple molecular pathways, such as immune cell activation and proinflammatory cytokine release.[8–10] Existing therapies against AQP4-ON focus on improving symptoms associated with acute attacks and preventing further relapses. An acute attack is typically treated with intravenous methylprednisolone injection or plasma exchange. Moreover, maintenance using immunomodulatory drugs is recommended to prevent relapse during the remission phase.[11,12] Eculizumab (targeting complement C5), inebilizumab (targeting CD19), and satralizumab (targeting IL-6) are some selective and potentially therapeutic drugs against AQP4-ON.[13,14] However, AQP4-ON pathogenesis remains unclear; thus, it is imperative to elucidate the mechanism underlying acute attack.

The transcription levels of genes in cells or tissues are studied using transcriptomics. Recently, this technique has been extensively used to systematically analyze changes in gene expression associated with various diseases, including cancer and autoimmune, cardiovascular, and cerebrovascular diseases.[15–18] This approach helps elucidate molecular mechanisms underlying these diseases, thereby contributing to understanding them and developing treatment strategies against them. Previously, we found that AQP4-ON and MOG-ON exhibit different immune mechanisms, and *TSPO* may be an important target for AQP4-ON.[19,20] Herein, the peripheral whole blood of patients with AQP4-ON in the acute and remission phase was collected and subjected to RNA sequencing (RNA-seq) in order to elucidate different immune mechanisms during acute onset and remission status. Additionally, the association of key molecules with vision prognosis was investigated.

Materials and Methods

Patients and Samples

We recruited 6 patients with AQP4-ON in the acute phase and 6 patients with AQP4-ON in the remission phase at the Affiliated Wuxi Clinical College of Nantong University from September 2021 to September 2022. AQP4-ON was diagnosed as per the guidelines of the Optic Neuritis Treatment Trial study.[21] Serum AQP4 antibody levels were measured using an enzyme-linked immunosorbent assay kit (RSR Ltd., UK) according to a previous study,[22] and results equal to 3.0 u/mL were considered positive. Patients with neurological diseases, such as encephalitis and myelitis, and eye diseases except cataracts, such as glaucoma, uveitis, and ischemic optic neuropathy, were excluded. Peripheral blood samples were collected before steroid treatment (acute phase) and during outpatient visits six months later (remission phase). We collected peripheral blood from two patients in both phases. Remission was defined as improvement in vision, relief from symptoms that remained stable for at least 30 days[23] and more than 90 days after the initial onset or more than 30 days before relapse.[24] Best corrected visual acuity (BCVA) was presented as logMAR for statistical analysis. The study was approved by the Ethics Committee of the Affiliated Wuxi Clinical College of Nantong University (No.2021Y-33), Follow the Declaration of Helsinki, and all patients signed an informed consent form (Table 1).

Table 1 Treatment and Prognosis of Patients

Patient ID	Sample	Affected Eyes	BCVA at Attendance	Last Follow-Up BCVA	AQP4-IgG Titer	Treatment Status at Time of Sampling
Acute stage						
Patient 1	A1	Right	2	3.5	>80	-
Patient 2	A2	Left	0.9	2.5	>80	-
Patient 3	A3	Left	1.7	2	10.37	-
Patient 4	A4	Right	0.6	0	40.83	-
Patient 5	A5	Left	2	0.1	>80	(Second onset, first onset was a year ago) IVMP and oral prednisolone and discontinued 7 months ago
Patient 6	A6	Right	2.5	1.4	>80	(Second onset, first onset was two years ago) IVMP and oral prednisolone and discontinued over one year ago

(*Continued*)

Table 1 (Continued).

Patient ID	Sample	Affected Eyes	BCVA at Attendance	Last Follow-Up BCVA	AQP4-IgG Titer	Treatment Status at Time of Sampling
Remission stage						
Patient 2	R1	Left	2.5	2.5	1.5	Mycophenolate mofetil and IVMP, oral prednisolone
Patient 7	R2	Right	0.3	0.4	>80	Mycophenolate mofetil and IVMP, oral prednisolone
Patient 8	R3	Right	1.8	1.7	15.14	IVMP and oral prednisolone
Patient 9	R4	Right	1.2	1.4	5.82	IVMP and oral prednisolone
Patient 10	R5	Left	0.2	0.2	3.32	IVMP and oral prednisolone
Patient 6	R6	Right	1.4	1.4	>80	IVMP and oral prednisolone

Notes: BCVA: Snellen visual acuity was converted to logarithm of the minimum angle of resolution (logMAR). Counting fingers vision was converted to a value of 2.0 logMAR, hand motion vision was converted to a value of 2.5 logMAR, light perception vision was converted to a value of 3.0 logMAR and no light perception vision was converted to a value of 3.5 logMAR. Underline indicates common patients in different periods of the acute and remission stage.
Abbreviation: IVMP, intravenous pulses of methylprednisolone.

RNA Extraction and Library Construction

The peripheral blood samples (2 mL) were collected from the patients in a special Vacutainer of EDTA for anticoagulation. Then, 4 mL of Trizol (Beyotime, Nantong, China) was added and stored at −80°C for unified testing. Total RNA was extracted using the TRIzol method following the standard TRIzol RNA extraction protocol. After confirming RNA integrity, it was reverse-transcribed into complementary DNA (cDNA). Subsequently, AMPure XP beads were used to selectively obtain cDNA fragments ranging from 250 to 300 bp in size (Beckman Coulter, Brea, California, USA). Following polymerase chain reaction, cDNA libraries were constructed using AMPure XP beads again. Quality control was performed using Agilent 2100 Bioanalyzer (Agilent Technologies Inc., Santa Clara, California, USA), and sequencing was performed on the Illumina NovaSeq 6000 platform (Illumina Inc., San Diego, California, USA).

RNA-Seq and Differentially Expressed Gene (DEG) Analysis

After preprocessing the data obtained, including quality control, removing low-quality sequences, and trimming adapter sequences, clean reads were aligned to a reference genome or transcriptome to obtain the expression counts for each gene. The raw data have been submitted to SRA and GEO database (accession numbers: PRJNA1172411, GSE217410). The samples were compared and DEGs were identified using statistical methods such as DESeq2 or edgeR. Genes with $P \leq 0.05$ adjusted by DESeq2 were considered differentially expressed.

Biological Function Analysis

Gene ontology (GO) enrichment and Kyoto Encyclopedia of Genes and Genomes (KEGG) pathway enrichment analyses were performed on the DEGs using the cluster Profiler R package (3.8.1). GO terms and KEGG pathways were considered significantly enriched at $P < 0.05$. Then we used STRING (http://string-db##or) to predict the interaction among the DEGs and Cytoscape 3.9.0 to construct a protein–protein interaction (PPI) network and calculate the degree of connectivity.

Immunocyte Infiltration Analysis

We used CIBERSORTx (https://cibersortx.stanford.edu) to analyze the differential expression of 22 immune cell subsets. Additionally, we used the Immune Cell Abundance Identifier (ImmuCellAI) gene set signature-based method (http://bioinfo.life.hust.edu.cn/ImmuCellAI#!/) to estimate the proportion of infiltrated immune cell types.

Statistical Analysis

Statistical analyses were performed using IBM SPSS Statistics 26.0. software for macOS (IBM Corporation, Armonk, NY, USA) and GraphPad Prism 9 software (GraphPad Software Inc., San Diego, CA, USA). For statistics, BCVA was presented as logMAR; BCVA of count fingers, hand motion, light perception, and no light perception were assigned to logMAR values of 2, 2.5, 3.0, and 3.5, respectively. A statistical analysis of differences was performed using the one-way analysis of variance

test or the Kruskal–Wallis test. Spearman correlation analysis was performed to evaluate the correlation between the data and vision. Data are expressed as the mean ± standard deviation or median. $P < 0.05$ was considered statistically significant.

Results

Demographic and Clinical Features of Patients

Ten patients with AQP4-ON and seven healthy controls (HCs) were recruited. The AQP4-ON group included six patients with acute phase (A) and six patients with remission phase (R) (peripheral blood from two patients was collected in both phases). The average age was 42.83±15.73 years in the A group and 37.33±16.50 years in the R group (P =0.57). The female/male ratio was 6/0 in the A group and 5/1 in the R group (P = 0.34). The BCVA was 1.62±0.72 logMAR in the A group and 1.25±0.88 logMAR in the R group (P = 0.44). The intraocular pressure was 16.82±6.08 mmHg in the A group and 14.44±3.39 mmHg in the R group (P = 0.42). The AQP4-IgG titer was 61.87±29.70 u/mL in the A group and 30.96±38.27 u/mL in the R group (P = 0.15). No significant differences were observed between the HCs and the patients regarding the age and sex ratio (P = 0.92 and P = 0.39, respectively; Tables 1 and 2).

Libraries Construction and Sequencing

The whole blood samples of three groups were subjected to RNA-Seq. High-throughput RNA-Seq was generated between 6.19 and 7.1 Gb of clean base reads from each library (Table 3). After stringent filtering of low-quality reads, 44,472,188 clean reads were obtained with quality scores > Q30, which accounted for > 89.06% of the reads, which were subsequently mapped to the reference genome. The aligned ratios of the reads ranged from 91.70% to 97.92% among nineteen libraries, and 53.04%–78.68% of the reads were uniquely mapped (Table 3). These data represented a high sequencing depth and quality sufficient for further transcriptomics analysis.

Summary of RNA-Seq Data and Disparities in Gene Expression Patterns

Principal component analysis (PCA) identified outlier samples and evaluated sample repeatability. No significant difference was observed among the three groups (Figure 1A). The Venn diagram showed 47 repetitive DEGs among the three groups (Figure 1B), and the cluster heatmap showed the differences in gene expression patterns among the three groups (Figure 1C). Specifically, 2646 DEGs were found between the A and HC groups, of which 834 were downregulated and 1812 were upregulated (Figure 2A). In total, 1883 DEGs were found between the R and HC groups, of which 713 were downregulated and 1170 were upregulated (Figure 2B).

GO and KEGG pathway enrichment analyses were performed. In the GO enrichment analysis of the acute phase, terms such as “cytokine receptor activity”, “dioxygenase activity”, and “Toll-like receptor binding” were enriched in the GO molecular function (MF) domain. Terms such as “neutrophil-mediated immunity”, “granulocyte activation”, and “neutrophil activation” were enriched in the GO biological process (BP) domain (Figure 2C). In the GO enrichment analysis of the remission phase, terms such as “chromatin binding”, “microtubule binding” and “histone binding” were enriched in the GO MF domain. Terms such as “nuclear chromosome segregation”, “chromosome segregation”, and “sister chromatid segregation” were enriched in the GO BP domain (Figure 2D). In the KEGG pathway enrichment

Table 2 Characteristics of Subjects with AQP4-ON and Healthy Control (HC)

	A (n=6)	R (n=6)	Total (n=10)	HC (n=7)	P^1	P^2
Age (years)	42.83±15.73	37.33±16.50	40.70±17.11	41.42±3.99	0.57	0.92
Sex (female/male)	6/0	5/1	9/1	5/2	0.34	0.39
BCVA(logMAR)	1.62±0.72	1.25±0.88	–	–	0.44	–
IOP (mmHg)	16.82±6.08	14.44±3.39	–	–	0.42	–
AQP4-IgG titer (u/mL)	61.87±29.70	30.96±38.27	-	-	0.15	-

Notes: P^1: Comparison between acute AQP4-ON and remission AQP4-ON. P^2: Comparison between total AQP4-ON and healthy control. All statistical values are expressed as the mean ± standard deviation (SD) unless otherwise indicated.

Abbreviations: BCVA, best-corrected visual acuity; IOP, intra-ocular pressure.

Table 3 Statistical Results of the RNA-Seq Date

Classification	Maximum	Minimum	Average
Clean reads (n)	47,365,186	41,285,976	44,472,188
Clean bases (G)	7.10	6.19	6.67
Q30 (%)	94.69	89.06	92.31
Reads aligned (%)	97.92	91.70	95.21
Unique map (%)	78.68	53.04	64.70

Notes: Clean base=Clean reads150bp. Q30: the percentage of data/bases with a Phred quality score > 30. Phred quality score > 30 means > 99.9% base call accuracy.

analysis of the acute phase, mitogen-activated protein kinase (MAPK) signaling, chemokine signaling, and Kaposi sarcoma-associated herpesvirus infection pathways were significantly enriched (Figure 2E). In the KEGG pathway enrichment analysis of the remission phase, cell cycle pathway was significantly enriched for the DEGs (Figure 2F).

Finally, the PPI network analysis of the DEGs among the three groups was performed using STRING and Cytoscape (Figure 3). The results revealed *TSPO* as the core gene that interacted most frequently in the acute phase and *CDK1* as the core gene in the remission phase. *TSPO* was considered an excellent target for treating diseases associated with neuroinflammation. Thus, *TSPO* might be an important target for treating acute AQP-ON. Additionally, *CDK1* played an important role during AQP4-ON remission.

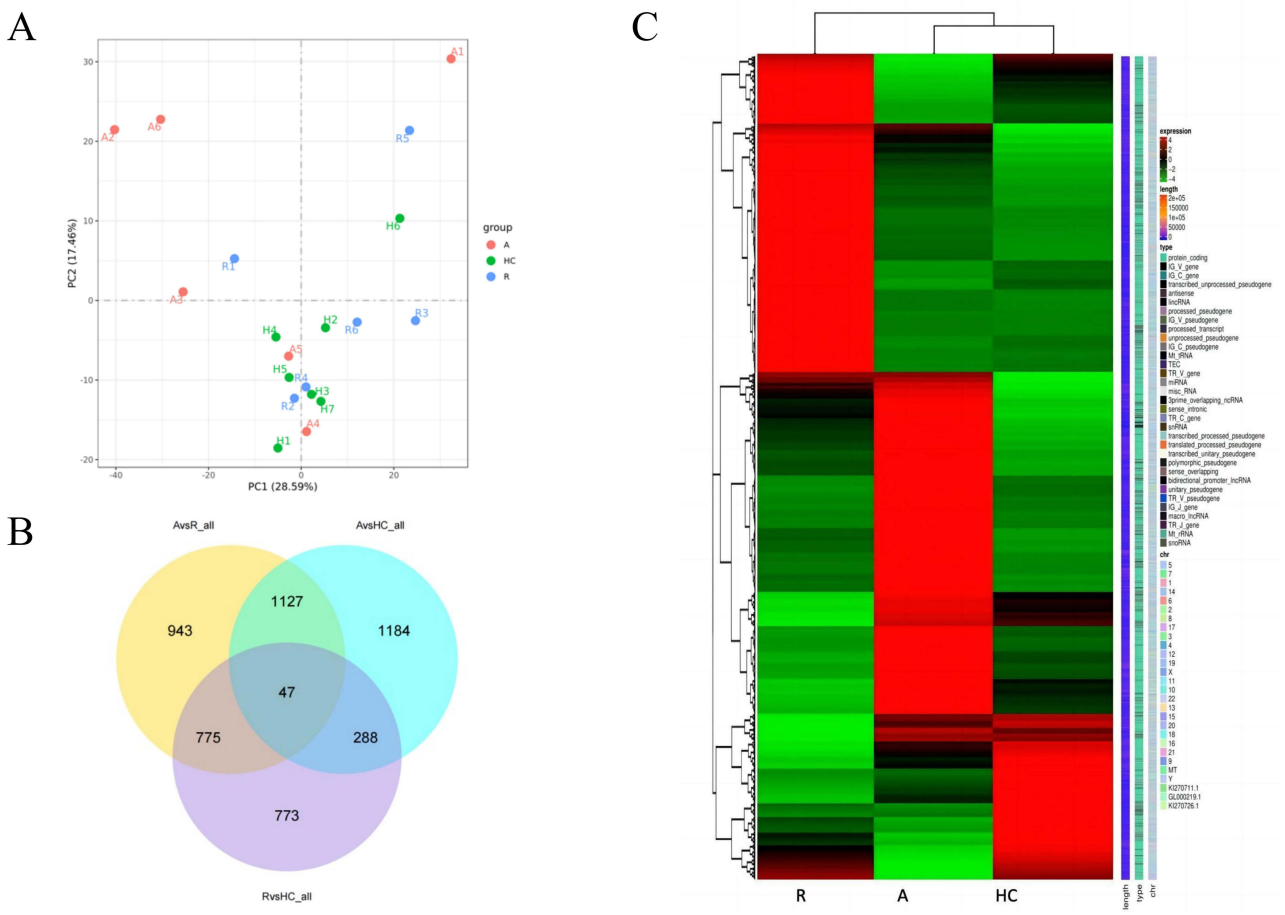

Figure 1 Functional enrichment analysis of acute stage (A) group, remission stage (R) group and healthy control (HC) group. (**A**) PCA analysis of three groups. (**B**) Venn diagram of three groups. (**C**) Heat map of three groups.

https://doi.org/10.2147/JIR.S507083

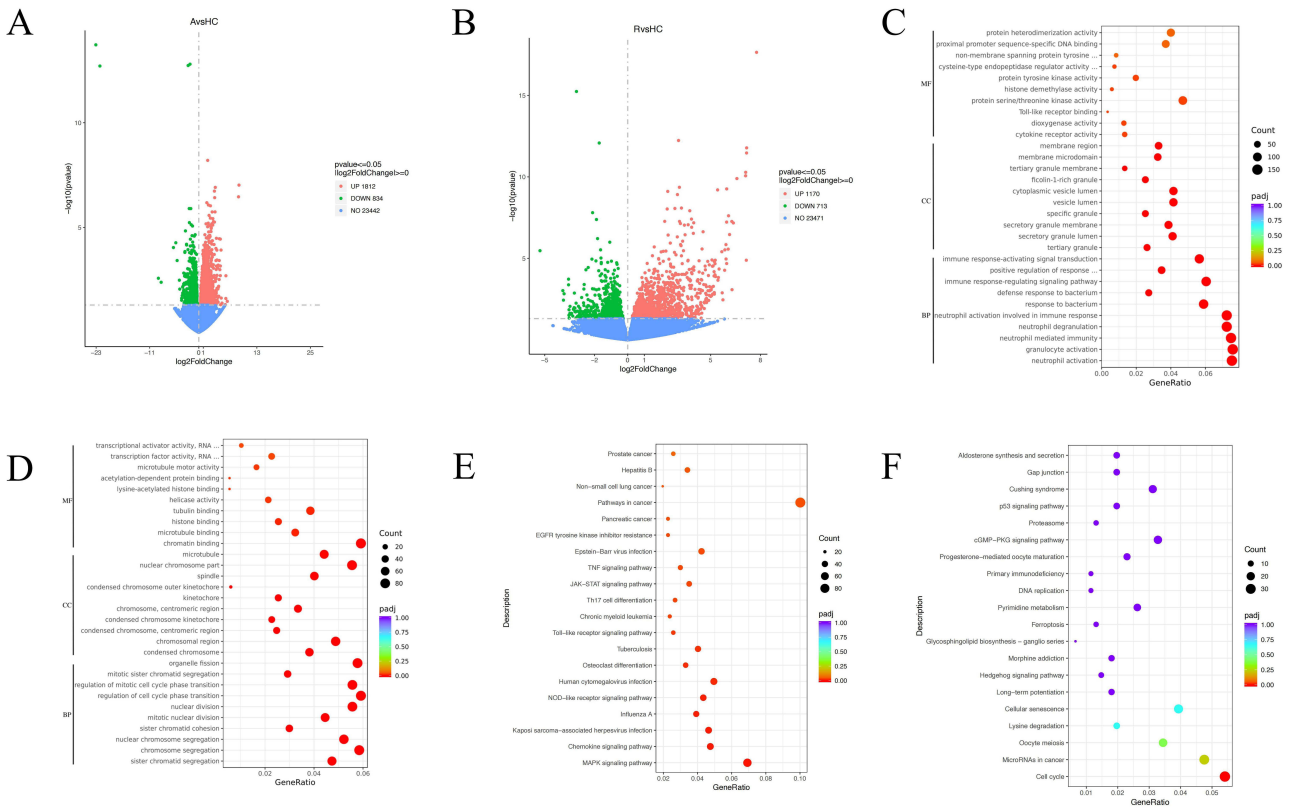

Figure 2 Differential gene expression analysis. (**A**) Volcano diagram of the differential expression gene in A group and HC group. (**B**) Volcano diagram of the differential expression gene in R group and HC group. (**C**) GO term enrichment analysis in A group and HC group. (**D**) GO term enrichment analysis in R group and HC group. (**E**) KEGG enrichment analysis in A group and HC group. (**F**) KEGG enrichment analysis in R group and HC group.

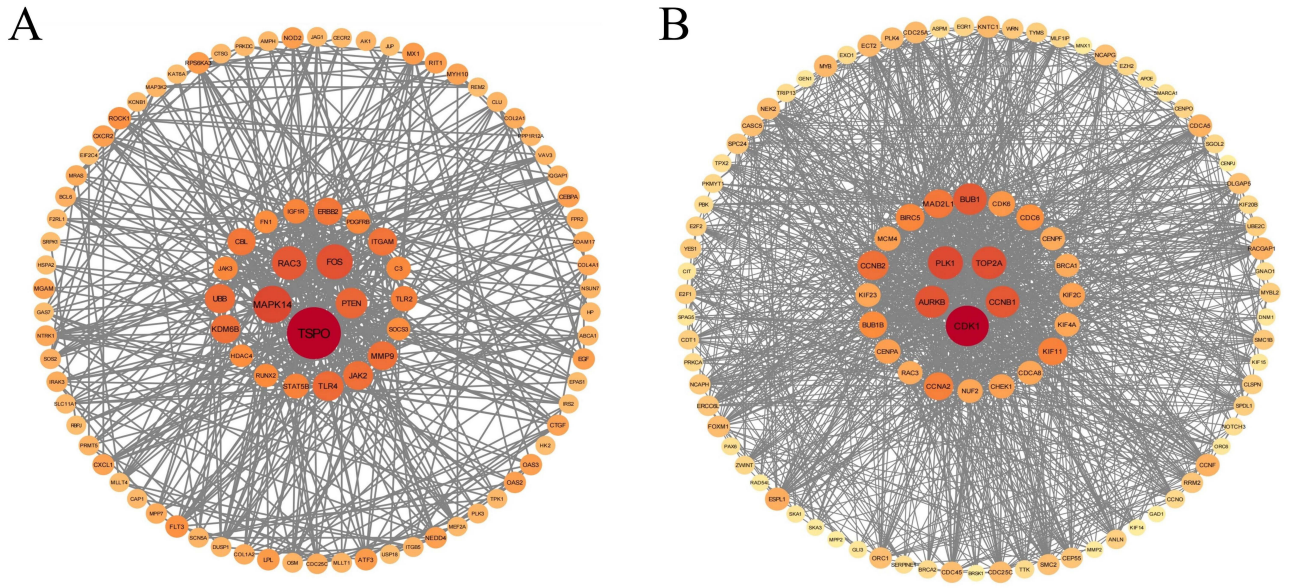

Figure 3 PPI network analysis of different genes. (**A**) PPI network analysis of different genes in A group and HC group. (**B**) PPI network analysis of different genes in R group and HC group.

Cell-Type Enrichment Analysis Based on Gene Expression Signature

Twenty-two types of infiltrating immune cells in the three groups were estimated using CIBERSORT. The PCA results showed significant differences in infiltrating immune cells among the three groups (Figure 4A). After removing three

subtypes of infiltrating immune cells (M1 macrophages, activated mast cells, and eosinophils), the proportion of other infiltrating immune cell subtypes in each group was determined. Significant differences were observed in the proportion of immune cells between the A and R groups. The proportion of immune cells was similar between the R and HC groups (Figure 4B and C). Except for A4 and A5, the proportion of B cells in the remaining samples in the A group was higher than that in the HC group, and B cells were almost completely depleted in the R group. Except for R2, which showed the highest proportion of CD8 T cells, and A1, which had the highest proportion of Monocytes, the remaining samples in the three groups showed the highest proportion of neutrophils (Figure 4B).

Correlation Analysis Between Infiltrating Immune Cells and Visual Acuity at the Last Follow-Up

Correlation analysis was performed between the immune cell infiltration proportion calculated by CIBERSORT and the BCVA converted to logMAR at the last follow-up. The BCVA was positively correlated with activated CD4 memory T cells (rs=0.8053, P=0.054) and resting NK cells (rs=0.5828, P=0.2248), and negatively correlated with neutrophils (rs=0.1644, P=0.7556) in the A group (Figure 5A). Moreover, the BCVA was negatively correlated with monocytes (rs=0.6922, P=0.1276), CD8 T cells (rs=0.5571, P=0.2508), and M0 macrophages (rs=0.6922, P=0.1276) and positively correlated with neutrophils (rs=0.474, P=0.3422) (Figure 5B) in the R group. Furthermore, correlation analysis was performed between *TSPO* gene expression and immune cell infiltration proportion to evaluate *TSPO* gene expression and vision prognosis. In all AQP4-ON samples, *TSPO* was positively correlated with M0 macrophages (rs=0.4794, P=0.1145) and neutrophils (rs=0.5267, P=0.0784), whereas it was negatively correlated with CD8 T cells (rs=0.66, P=0.0195), and resting NK cells (rs=0.6662, P=0.0180) (Figure 5C). Therefore, the proportion of immune cells reflected the AQP4-ON disease status, and neutrophils, memory B cells, naïve B cells, and CD8 T cells played crucial roles in AQP4-ON occurrence and development.

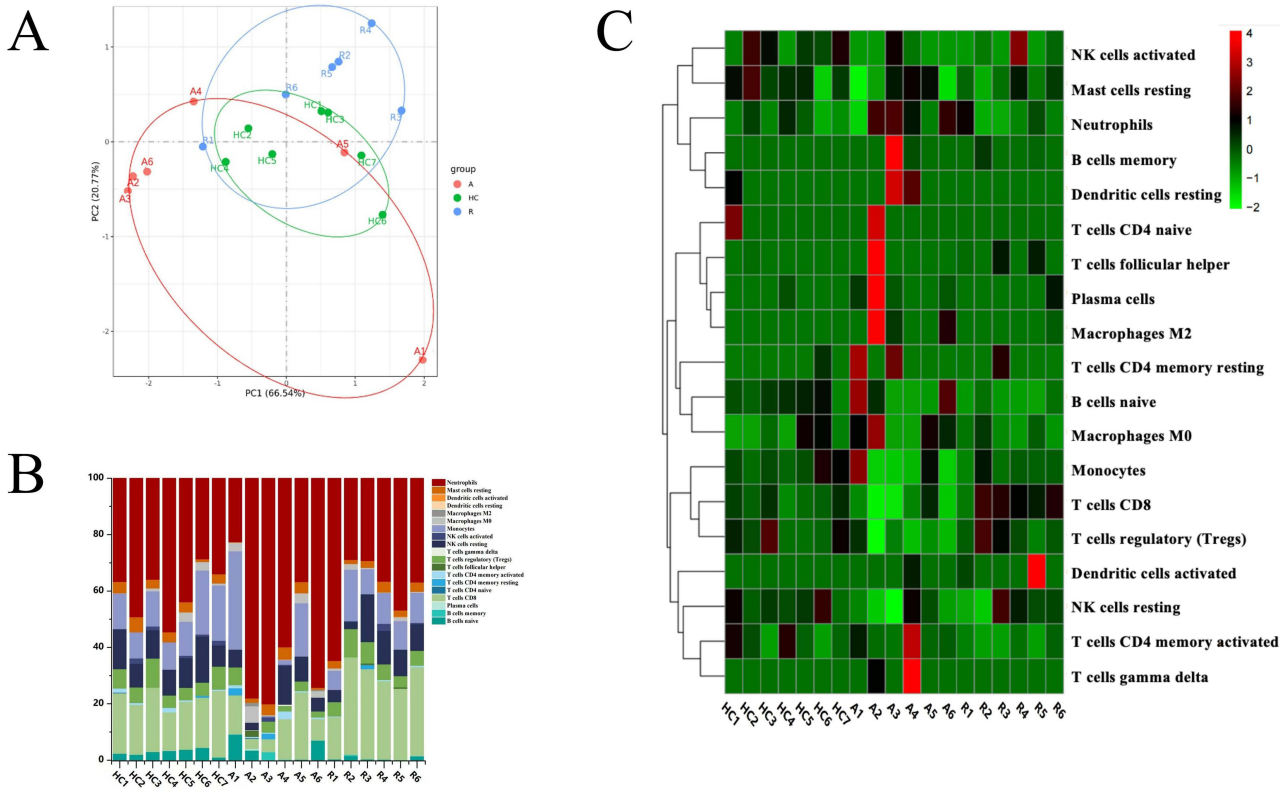

Figure 4 Analysis of immune cell infiltration. (**A**) PCA analysis of infiltrating immune cells. (**B**) Cumulative histogram of the proportion of 22 infiltrating immune cells in each sample, and the total proportion of the 22 infiltrating immune cells is equal to 100%. (**C**) Heat map of 22 infiltrating immune cells in each sample.

https://doi.org/10.2147/JIR.S507083

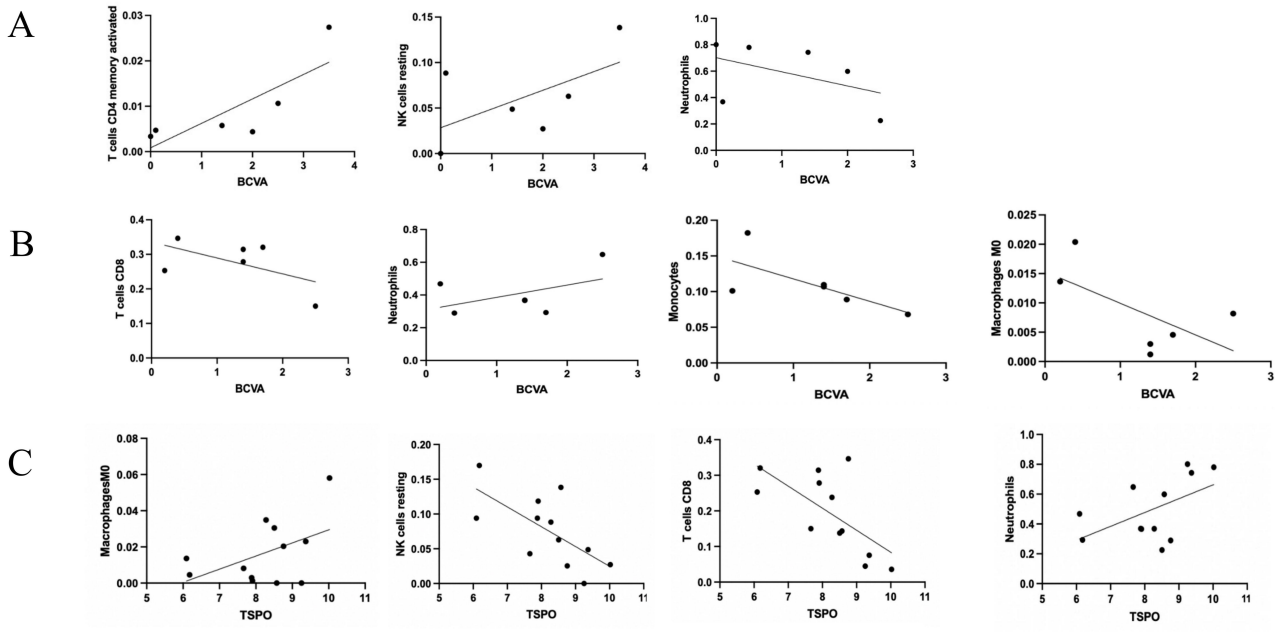

Figure 5 Correlation analysis. (**A**) Spearman correlation analysis between infiltrating immune cell proportion and BCVA at last follow-up in A group. (**B**) Spearman correlation analysis between infiltrating immune cell proportion and BCVA at last follow-up in R group. (**C**) Spearman correlation analysis between infiltrating immune cell proportion and TSPO gene expression in AQP4-ON.

Discussion

Currently, no consensus exists in the literature regarding the timing of the acute and remission phases of AQP4-ON. However, some discussions are available regarding the acute and remission phases of NMOSD. The acute phase is the period characterized by the acute onset of symptoms lasting less than one month. Conversely, the remission phase encompasses two distinct types as follows: the attack remission phase, characterized by symptoms with an acute onset lasting more than one month, and the remission phase, characterized by no recurrence within a month.[25,26] In addition, it has been described that the remission period is more than 90 days after the initial onset or more than 30 days before relapse.[24] Herein, all patients in the acute phase were evaluated within one month of symptom onset, and the samples were collected before treatment initiation. All subjects in the remission period were mainly more than 90 days after the initial onset or more than 30 days before relapse. A correlation has been observed between antibody levels and disease activity in various autoimmune diseases, including systemic lupus erythematosus, where frequently decreased antibody titers were regarded as an indicator of disease remission.[27] During the remission phase, the dampened immune response in the body gradually reduces antibody levels.

RNA-Seq was performed to analyze the immune response in AQP4-ON at the whole blood level. A significant difference was observed between the onset and remission of AQP4-ON, suggesting that the immune system played different roles at different phases of this disease. During the acute phase, inflammatory and innate immunity-related pathways, including MAPK signaling, Toll-like receptor, and chemokine receptor signaling pathways, and neutrophil-mediated activity were significantly upregulated. This phenomenon is consistent with the previous understanding of the ON pathological mechanism that immune cells play an important role in inflammation-mediated tissue damage. The proinflammatory environment caused by neutrophil preactivation promotes astrocyte destruction, and complement activation triggered by AQP4-IgG binding to astrocytes plays a key role in exclusive neutrophil recruitment and activation in NMOSD.[28] Moreover, cell cycle-related pathways and chromosome-related activities were significantly upregulated during remission. The expression of immune-related genes was significantly downregulated compared with that during the acute onset phase. Additionally, the degree of the activation of signaling pathways related to immune activation was significantly weakened, which suggested that immune cells exhibit regulatory properties during remission.

Chemokine receptor signaling pathways are upstream of the MAPK signaling pathway.[29] Toll-like receptors play an essential role in AQP4-ON.[30] Chemokines and chemokine receptors play a pro-inflammatory role in autoimmune diseases;[31] however, their mechanisms in AQP4-ON remain unknown. The significant upregulation of cell cycle signaling pathways during the remission phase may be associated with the repair of cell tissues after inflammation is alleviated. Thus, the roles of these signaling pathways in AQP4-ON need further investigation.

In addition to neutrophils, B and NK cells play a role in the acute phase of AQP4-ON. NK cells are associated with antibody-dependent cell-mediated cytotoxicity in AQP4-ON pathogenesis, and B cells produce pathogenic AQP4 antibodies.[32,33] Additionally, activated CD4 memory T cells, CD8 T cells, monocytes, M0 macrophages, and Tregs may contribute to AQP4-ON pathogenesis. CD4 memory T-cell activation plays a critical role in mediating immune responses in autoimmune diseases.[34] In systemic lupus erythematosus, CD4 memory T-cell activation is associated with DNA methylation regulation, and DNA hypomethylation facilitates proinflammatory gene expression.[35] Similar to activated CD4 memory T cells, CD8 T cells contribute to the immunopathology of chronic autoimmune diseases.[34] Tregs maintain immune homeostasis and may exert a protective effect on autoimmune diseases.[36,37] During AQP4-ON remission, Treg depletion may regulate immune functions. Herein, in the acute phase of AQP4-ON, the higher proportion of neutrophils was associated with the lower proportion of monocytes, and the lower proportion of B cells was associated with a better visual prognosis. This was confirmed by the good visual prognosis of A4 and A5. In the present samples, the proportion of neutrophils in the acute phase increased, the proportion of CD8 T cells decreased, and the proportion of B cells, A4, and A5 increased. Additionally, individual analysis explained these differences and the relationship between immune cells and visual prognosis; however, a few studies have focused on this aspect. The role of AQP4-IgG in AQP4-ON pathogenesis remains unclear. AQP4-IgG is probably produced when the protein of the infectious agent well mimics the antibody target,[38] thus indicating that pathogen infection may affect AQP4-IgG production. Nevertheless, upregulated *TSPO* expression may be induced by inflammatory mediators released from immune cells and other inflammation-related cells but does not necessarily represent a simple proinflammatory state.[39,40] In an infection-mediated mouse model, cytokine gene expression was upregulated, whereas *TSPO* expression was downregulated.[40] Thus, its underlying mechanism needs further investigation. Herein, upregulated *TSPO* expression was probably beneficial for visual prognosis in patients with AQP4-ON. *TSPO* expressed mainly by neutrophils probably played a role in the acute phase of AQP4-ON and an increase in the number of neutrophils in ON implied the efficient clearance of inflammatory pathogens, local control of inflammation, and protection and repair of nerve cells.

Nevertheless, this study has several limitations. Owing to the rarity of the disease and the relatively poor prognosis the sample size is small. Thus, the present findings should be validated by more studies with larger sample sizes. Furthermore, the samples used in the study may not be representative of the entire patient population with AQP4-ON. This may lead to inaccuracies and limit the generalizability of the results. Additionally, gene expression in peripheral blood may be perturbed by many external factors.

Conclusion

In conclusion, the difference in immune cell infiltration between the acute and remission phases has potential implications for visual prognosis. Decreased AQP4 antibody titers during remission are accompanied by the resolution of innate immune-related pathways and inflammation-related effects and the activation of the cell cycle, which may have implications in developing treatment strategies.

Acknowledgments

Thanks to everyone who contributed to this article.

Disclosure

The author(s) report no conflicts of interest in this work.

References

1. Cruz-Herranz A, Dietrich M, Hilla AM, et al. Monitoring retinal changes with optical coherence tomography predicts neuronal loss in experimental autoimmune encephalomyelitis. *J Neuroinflammation*. 2019;16(1):203. doi:10.1186/s12974-019-1583-4
2. Hoshino Y, Noto D, Sano S, et al. Dysregulated B cell differentiation towards antibody-secreting cells in neuromyelitis optica spectrum disorder. *J Neuroinflammation*. 2022;19(1):6. doi:10.1186/s12974-021-02375-w
3. Abdel-Mannan O, Klein A, Bachar Zipori A, et al. Radiologically isolated aquaporin-4 antibody neuromyelitis optica spectrum disorder. *Mult Scler*. 2022;28(4):676–679. doi:10.1177/13524585221074947
4. Morita Y, Itokazu T, Nakanishi T, Hiraga SI, Yamashita T. A novel aquaporin-4-associated optic neuritis rat model with severe pathological and functional manifestations. *J Neuroinflammation*. 2022;19(1):263. doi:10.1186/s12974-022-02623-7
5. Kim SH, Mealy MA, Levy M, et al. Racial differences in neuromyelitis optica spectrum disorder. *Neurology*. 2018;91(22):e2089–e2099. doi:10.1212/WNL.0000000000006574
6. Tang J, Zeng X, Yang J, et al. Expression and clinical correlation analysis between repulsive guidance molecule a and neuromyelitis optica spectrum disorders. *Front Immunol*. 2022;13:766099. doi:10.3389/fimmu.2022.766099
7. Liu C, Shi M, Zhu M, Chu F, Jin T, Zhu J. Comparisons of clinical phenotype, radiological and laboratory features, and therapy of neuromyelitis optica spectrum disorder by regions: update and challenges. *Autoimmun Rev*. 2022;21(1):102921. doi:10.1016/j.autrev.2021.102921
8. Yao X, Verkman AS. Marked central nervous system pathology in CD59 knockout rats following passive transfer of neuromyelitis optica immunoglobulin G. *Acta Neuropathol Commun*. 2017;5(1):15. doi:10.1186/s40478-017-0417-9
9. Ratelade J, Asavapanumas N, Ritchie AM, Wemlinger S, Bennett JL, Verkman AS. Involvement of antibody-dependent cell-mediated cytotoxicity in inflammatory demyelination in a mouse model of neuromyelitis optica. *Acta Neuropathol*. 2013;126(5):699–709. doi:10.1007/s00401-013-1172-z
10. Tradtrantip L, Yao X, Su T, Smith AJ, Verkman AS. Bystander mechanism for complement-initiated early oligodendrocyte injury in neuromyelitis optica. *Acta Neuropathol*. 2017;134(1):35–44. doi:10.1007/s00401-017-1734-6
11. Naphattalung Y, Chuenkongkaew WL, Chirapapaisan N, Laowanapiban P, Sawangkul S. Plasma exchange for acute optic neuritis in neuromyelitis optica or neuromyelitis optica spectrum disorder: a systematic review. *Ann Med*. 2023;55(1):2227422. doi:10.1080/07853890.2023.2227422
12. Huang TL, Lin KH, Wang JK, Tsai RK. Treatment strategies for neuromyelitis optica. *Ci Ji Yi Xue Za Zhi*. 2018;30(4):204–208.
13. Mora Cuervo DL, Hansel G, Sato DK. Immunobiology of neuromyelitis optica spectrum disorders. *Curr Opin Neurobiol*. 2022;76:102618. doi:10.1016/j.conb.2022.102618
14. Carnero Contentti E, Correale J. Neuromyelitis optica spectrum disorders: from pathophysiology to therapeutic strategies. *J Neuroinflammation*. 2021;18(1):208. doi:10.1186/s12974-021-02249-1
15. Montaner J, Ramiro L, Simats A, et al. Multilevel omics for the discovery of biomarkers and therapeutic targets for stroke. *Nat Rev Neurol*. 2020;16(5):247–264. doi:10.1038/s41582-020-0350-6
16. Sun L, Yu F, Yi F, et al. Acteoside from ligustrum robustum (Roxb.) Blume ameliorates lipid metabolism and synthesis in a HepG2 cell model of lipid accumulation. *Front Pharmacol*. 2019;10:602. doi:10.3389/fphar.2019.00602
17. Huang Z, Xie L, Xu Y, et al. Essential oils from Zingiber striolatum Diels attenuate inflammatory response and oxidative stress through regulation of MAPK and NF-κB signaling pathways. *Antioxidants*. 2021;10(12):2019.
18. Zafari N, Bathaei P, Velayati M, et al. Integrated analysis of multi-omics data for the discovery of biomarkers and therapeutic targets for colorectal cancer. *Comput Biol Med*. 2023;155:106639. doi:10.1016/j.compbiomed.2023.106639
19. Werry EL, Bright FM, Piguet O, et al. Recent developments in TSPO PET imaging as a biomarker of neuroinflammation in neurodegenerative disorders. *Int J Mol Sci*. 2019;20(13):3161. doi:10.3390/ijms20133161
20. Chen Z, Haider A, Chen J, et al. The repertoire of small-molecule PET probes for neuroinflammation imaging: challenges and opportunities beyond TSPO. *J Med Chem*. 2021;64(24):17656–17689. doi:10.1021/acs.jmedchem.1c01571
21. Beck RW, Cleary PA, Anderson MM, et al. A randomized, controlled trial of corticosteroids in the treatment of acute optic neuritis. The optic neuritis study group. *N Engl J Med*. 1992;326(9):581–588. doi:10.1056/NEJM199202273260901
22. De Lott LB, Burke JF, Andrews CA, et al. Association of individual-level factors with visual outcomes in optic neuritis: secondary analysis of a randomized clinical trial. *JAMA Network Open*. 2020;3(5):e204339. doi:10.1001/jamanetworkopen.2020.4339
23. Yang X, Peng J, Huang X, et al. Association of circulating follicular helper T cells and serum CXCL13 with neuromyelitis optica spectrum disorders. *Front Immunol*. 2021;12:677190. doi:10.3389/fimmu.2021.677190
24. Jitprapaikulsan J, Fryer JP, Majed M, et al. Clinical utility of AQP4-IgG titers and measures of complement-mediated cell killing in NMOSD. *Neurol Neuroimmunol Neuroinflamm*. 2020;7(4). doi:10.1212/NXI.0000000000000727
25. Tong Y, Liu J, Yang T, et al. Association of pain with plasma C5a in patients with neuromyelitis optica spectrum disorders during remission. *Neuropsychiatr Dis Treat*. 2022;18:1039–1046. doi:10.2147/NDT.S359620
26. Yang H, Han L, Zhou YJ, et al. Lower serum interleukin-22 and interleukin-35 levels are associated with disease status in neuromyelitis optica spectrum disorders. *CNS Neurosci Ther*. 2020;26(2):251–259. doi:10.1111/cns.13198
27. Zhang H, Hu Q, Zhang M, et al. Bach2 deficiency leads to spontaneous expansion of IL-4-producing T follicular helper cells and autoimmunity. *Front Immunol*. 2019;10:2050. doi:10.3389/fimmu.2019.02050
28. Piatek P, Domowicz M, Lewkowicz N, et al. C5a-preactivated neutrophils are critical for autoimmune-induced astrocyte dysregulation in neuromyelitis optica spectrum disorder. *Front Immunol*. 2018;9:1694. doi:10.3389/fimmu.2018.01694
29. Ren Z, Wang W, Li J. Identifying molecular subtypes in human colon cancer using gene expression and DNA methylation microarray data. *Int J Oncol*. 2016;48(2):690–702. doi:10.3892/ijo.2015.3263
30. Chen X, Cheng L, Pan Y, et al. Different immunological mechanisms between AQP4 antibody-positive and MOG antibody-positive optic neuritis based on RNA sequencing analysis of whole blood. *Front Immunol*. 2023;14:1095966. doi:10.3389/fimmu.2023.1095966
31. Wasilko DJ, Johnson ZL, Ammirati M, et al. Structural basis for chemokine receptor CCR6 activation by the endogenous protein ligand CCL20. *Nat Commun*. 2020;11(1):3031. doi:10.1038/s41467-020-16820-6
32. Duan T, Smith AJ, Verkman AS. Complement-independent bystander injury in AQP4-IgG seropositive neuromyelitis optica produced by antibody-dependent cellular cytotoxicity. *Acta Neuropathol Commun*. 2019;7(1):112. doi:10.1186/s40478-019-0766-7

33. Hofmann K, Clauder AK, Manz RA. Targeting B cells and plasma cells in autoimmune diseases. *Front Immunol*. 2018;9:835. doi:10.3389/fimmu.2018.00835
34. Cheng C, Zhou J, Chen R, et al. Predicted disease-specific immune infiltration patterns decode the potential mechanisms of long non-coding RNAs in primary Sjogren's syndrome. *Front Immunol*. 2021;12:624614. doi:10.3389/fimmu.2021.624614
35. Zhang Y, Zhao M, Sawalha AH, Richardson B, Lu Q. Impaired DNA methylation and its mechanisms in CD4(+)T cells of systemic lupus erythematosus. *J Autoimmun*. 2013;41:92–99. doi:10.1016/j.jaut.2013.01.005
36. Kundu M, Mondal S, Roy A, Martinson JL, Pahan K. Sodium benzoate, a food additive and a metabolite of cinnamon, enriches regulatory T cells via STAT6-mediated upregulation of TGF-β. *J Immunol*. 2016;197(8):3099–3110. doi:10.4049/jimmunol.1501628
37. Mahne AE, Klementowicz JE, Chou A, Nguyen V, Tang Q. Therapeutic regulatory T cells subvert effector T cell function in inflamed islets to halt autoimmune diabetes. *J Immunol*. 2015;194(7):3147–3155. doi:10.4049/jimmunol.1402739
38. Tsymala I, Nigritinou M, Zeka B, et al. Induction of aquaporin 4-reactive antibodies in Lewis rats immunized with aquaporin 4 mimotopes. *Acta Neuropathol Commun*. 2020;8(1):49. doi:10.1186/s40478-020-00920-x
39. Notter T, Coughlin JM, Gschwind T, et al. Translational evaluation of translocator protein as a marker of neuroinflammation in schizophrenia. *Mol Psychiatry*. 2018;23(2):323–334. doi:10.1038/mp.2016.248
40. Da Silva T, Hafizi S, Watts JJ, et al. In vivo imaging of translocator protein in long-term cannabis users. *JAMA Psychiatry*. 2019;76(12):1305–1313. doi:10.1001/jamapsychiatry.2019.2516